Open Access Full Text Article

ORIGINAL RESEARCH

N⁶-Methyladenosine-Modified LEAWBIH Drives Hepatocellular Carcinoma Progression through Epigenetically Activating Wnt/β-Catenin Signaling

Huamei Wei[1,]*, Lizheng Huang[2,]*, Qi Lu[2,]*, Zheng Huang[2], Yanyan Huang[2], Zuoming Xu[3], Wenchuan Li[3], Jian Pu[3,4]

[1]Department of Pathology, Affiliated Hospital of Youjiang Medical University for Nationalities, Baise, People's Republic of China; [2]Graduate College of Youjiang Medical University for Nationalities, Baise, People's Republic of China; [3]Department of Hepatobiliary Surgery, Affiliated Hospital of Youjiang Medical University for Nationalities, Baise, People's Republic of China; [4]Guangxi Clinical Medical Research Center of Hepatobiliary Disease, Baise, People's Republic of China

*These authors contributed equally to this work

Correspondence: Jian Pu, Department of Hepatobiliary Surgery, Affiliated Hospital of Youjiang Medical University for Nationalities, No. 18 Zhongshan Two Road, Baise, 533000, People's Republic of China, Email jian_pu@126.com

Purpose: N⁶-methyladenosine (m⁶A) modification plays an important role in regulating RNA maturation, stability, and translation. Thus, m⁶A modification is involved in various pathophysiological processes including hepatocellular carcinoma (HCC). However, the direct contribution of m⁶A modifications to RNA function in HCC remains unclear. Here, we identified LEAWBIH (long non-coding RNA epigenetically activating Wnt/β-catenin signalling in HCC) as an m⁶A-modified long non-coding RNA (lncRNA) and investigated the effects of m⁶A on the function of LEAWBIH in HCC.

Methods: Quantitative polymerase chain reaction was performed to measure the gene expression in tissues and cells. The level of m⁶A modification was detected using a methylated RNA immunoprecipitation assay and single-base elongation- and ligation-based qPCR amplification method. Cell proliferation was evaluated using the Glo cell viability and CCK-8 assays. Cell migration and invasion were evaluated using Transwell migration and invasion assays. The mechanisms of m⁶A modified LEAWBIH were investigated using chromatin isolation by RNA purification, chromatin immunoprecipitation, and dual-luciferase reporter assays.

Results: LEAWBIH was highly expressed and correlated with poor survival in HCC patients. LEAWBIH was identified as a m⁶A-modified transcript. m⁶A modification increased LEAWBIH transcript stability. The m⁶A modification level of LEAWBIH was increased in HCC, and a high m⁶A modification level of LEAWBIH predicted poor survival. LEAWBIH promotes HCC cell proliferation, migration, and invasion in an m⁶A modification-dependent manner. Mechanistic investigations revealed that m⁶A-modified LEAWBIH activated Wnt/β-catenin signaling. m⁶A-modified LEAWBIH binds to the m⁶A reader YTHDC1, which further interacts with and recruits H3K9me2 demethylase KDM3B to *CTNNB1* promoter, leading to H3K9me2 demethylation and *CTNNB1* transcription activation. Functional rescue assays showed that blocking Wnt/β-catenin signaling abolished the role of LEAWBIH in HCC.

Conclusion: m⁶A-modified LEAWBIH exerts oncogenic effects in HCC by epigenetically activating Wnt/β-catenin signaling, highlighting m⁶A-modified LEAWBIH as a promising therapeutic target for HCC.

Keywords: hepatocellular carcinoma, N⁶-methyladenosine, histone methylation, Wnt/β-catenin signaling

Introduction

Liver cancer is the sixth most common malignancy and the third leading cause of cancer-related deaths worldwide.[1] Hepatocellular carcinoma (HCC) is the most common type of liver cancer.[2] Surgical resection and liver transplantation are the preferred therapies for early-stage HCCs.[3] For recurrent and advanced-stage HCCs, systemic therapies, including tyrosine kinase inhibitors, immune checkpoint inhibitors, and monoclonal antibodies, are currently utilized.[2] However, the prognosis of these advanced-stage HCCs is still very poor, with a 5-year survival rate of less than 20%.[4] Thus, further elucidation of the mechanisms driving HCC initiation and progression is urgently needed to develop more efficient treatments for HCC.

The pathophysiology of HCC has been gradually revealed.[5–9] Several prevalent genetic mutations have been frequently reported, such as TP53, TERT, AXIN1, APC, CTNNB1, CDKN2A, and RB1.[10] Apart to genetic mutations, more dysregulated expressed genes have also been identified.[11] Epigenetic aberrations are the major contributors to gene expression dysregulation.[12] Epigenetic modifications, which include DNA methylation, histone acetylation, histone methylation, and non-coding RNAs, can activate or repress gene transcription and expression by changing the chromatin structure.[13–18] Long non-coding RNAs (lncRNAs) are a class of non-coding RNAs with more than 200 nucleotides in length.[19–23] Aberrant expressions and functions of lncRNAs have been revealed in many diseases, including HCC.[24–28]

Recently, post-transcriptional RNA modifications, which are also known as epitranscriptomic modifications, have been found in various pathophysiological processes.[29,30] N[6]-methyladenosine (m[6]A) is the most common epitranscriptomic modification and has been intensively investigated.[31,32] Increasing evidence has shown that m[6]A modification plays important roles in modulating RNA fate, including RNA maturation, splicing, stability, and translation.[33–36] Thus, by regulating RNA fate, m[6]A modification shows critical functions in many diseases, including HCC.[37–39] m[6]A is catalyzed by m[6]A methyltransferases, such as METTL3, METTL14, and WTAP, and removed by m[6]A demethylases, such as FTO, ALKBH3, and ALKBH5.[40–42] Routinely, m[6]A is recognized by m[6]A readers, such as YTHDC1, HNRNPG, and YTHDF1, which mediate most of the roles of m[6]A in various pathophysiology processes.[43] However, the potential contributions of m[6]A modification to the roles and clinical significance of lncRNAs remain largely unclear.

In this study, by investigating The Cancer Genome Atlas (TCGA) Liver Hepatocellular Carcinoma (LIHC) RNA-seq data, we found that lncRNA RP4-773N10.4 (also named AL160006.1) was upregulated and associated with poor prognosis in HCC. Further investigation revealed that RP4-773N10.4 could be m[6]A modified. m[6]A-modified RP4-773N10.4 exerted oncogenic roles in HCC through epigenetic activation of Wnt/β-catenin signalling. Thus, we named RP4-773N10.4 as long non-coding RNA epigenetically activating Wnt/β-catenin signalling in HCC (LEAWBIH). We further investigated the mechanisms underlying the role of the m[6]A-modified LEAWBIH in HCC.

Materials and Methods
Patient Specimens
The correlation between LEAWBIH expression and prognosis, based on TCGA-LIHC RNA-seq data, was analyzed using the on line tool GEPIA (Gene Expression Profiling Interactive Analysis, http://gepia.cancer-pku.cn/).[44] Gene expression levels based on TCGA-LIHC RNA-seq data were download from https://portal.gdc.cancer.gov/. Furthermore, 73 pairs of HCC tissues and matched adjacent liver tissues were obtained from patients with HCC who underwent surgery at the Affiliated Hospital of Youjiang Medical University for Nationalities. Written informed consent was obtained from all participants. This study was conducted in accordance with the Declaration of Helsinki and was reviewed and approved by the Affiliated Hospital of Youjiang Medical University for Nationalities Institutional Review Board.

Cell Culture
The human immortalized liver cell line THLE-2 (cat. no. CRL-2706) was acquired from American Type Culture Collection (ATCC, Manassas, VA, USA). The human HCC cell line SK-HEP-1 (cat. no. TCHu109), HuH-7 (cat. no. SCSP-526) and Hep3B cells (cat. no. SCSP-5045) were obtained from the Chinese Academy of Sciences Cell Bank (Shanghai, China). THLE-2 cells were maintained using the BEGM Bullet Kit (cat. no. CC-3170; Lonza, Basel, Switzerland). SK-HEP-1 and Hep3B cells were maintained in Eagle's Minimum Essential Medium (Invitrogen, Carlsbad, CA, USA) supplemented with 10% fetal bovine serum (FBS, Invitrogen). HuH-7 cells were maintained in Dulbecco's modified Eagle's medium (DMEM; Invitrogen) supplemented with 10% FBS. All cells were cultured at 37°C and 5% CO_2 and routinely tested as mycoplasma-free.

RNA Isolation and Quantitative Polymerase Chain Reaction (qPCR)
Total RNA was isolated using the RNA Isolator Total RNA Extraction Reagent (Cat. no. R401; Vazyme, Nanjing, China), followed by being subjected to reverse transcription using HiScript III RT SuperMix for qPCR (cat. no. R323; Vazyme) to generate first-strand complementary DNA (cDNA). cDNA was subjected to quantitative polymerase chain reaction (qPCR)

using ChamQ Universal SYBR qPCR Master Mix (cat. no. Q711; Vazyme) on a QuantStudio Real-Time PCR Instrument (Applied Biosystems). Primer sequences were as follows:5'-TCAGAGCCAGCGTCAAGAC-3' (sense) and 5'-GCCCA CAAAGACACATCAGG-3' (antisense) for LEAWBIH; 5-CCACACCCTTCTCCAATCC-3' (sense) and 5'-GCTCCAC AGGCAAACTCATC-3' (antisense) for AXIN2; 5-CAGGTCAAACAGGAACATC-3' (sense) and 5'-TTTAGAGTACA CTCAGCAACG-3' (antisense) for LEF1; 5-ACAACTTCCTGTCCTACTACCG-3' (sense) and 5'-TCCTCCTCCTCT TCCTCCTC-3' (antisense) for CCND1; 5-CTTCCCCTACCCTCTCAA-3' (sense) and 5'-CGATTTCTTCCTCATCTTCT -3' (antisense) for MYC, 5'-AAACAGGAAGGGATGGAA-3' (sense) and 5'-CAGATGACGAAGAGCACAG-3' (antisense) for CTNNB1, 5'-ATCAAGTAGTGCCTCCAG-3' (sense) and 5'-CTTCCTCCTCATTCTCAG-3' (antisense) for YTHDC1, 5'-GCCTCCAACAACAAAACC-3' (sense) and 5'-CCATCACCATCTCCTTCAC-3' (antisense) for KDM3B, 5'-GTCGGAGTCAACGGATTTG-3' (sense) and 5'-TGGGTGGAATCATATTGGAA-3' (antisense) for GAPDH. GAPDH was used as an endogenous control. Relative expression was calculated using the comparative Ct method.

Detection of m⁶A Modification

The m⁶A-modified transcripts were enriched in methylated RNA immunoprecipitation (MeRIP) assays in HCC cells using the Magna MeRIP m⁶A Kit (cat. no. 17–10499, Millipore, Billerica, MA, USA). Enriched transcripts were measured using qPCR as described above. Furthermore, site-specific m⁶A modification was detected using the previously reported single-base elongation- and ligation-based qPCR amplification method (termed "SELECT").[45] Concurrent detections of non m⁶A-modified 2090 and 2672 sites were conducted, which served as input for m⁶A-modified 2095 and 2679 sites respectively. The probe sequences were as follows:5'-tagccagtaccgtagtgcgtgGCTTCCTCCA GACTTTGTCCAAG-3' (up) and 5'-5phos/CCATTGTCATCTCTCCAGCTAAGACcagaggctgagtcgctgcat-3' (down) for m⁶A 2095, 5'- tagccagtaccgtagtgcgtgCTCCAGACTTTGTCCAAGTCCAT-3' (up) and 5'-5phos/GTCATCTCTCCA GCTAAGACAGCTcagaggctgagtcgctgcat-3' (down) for A 2090, 5'-tagccagtaccgtagtgcgtgCTGCAGAACTCCCTGT GGGCCAG-3' (up) and 5'-5phos/CCAGGATCTGGGAGCCCTGGAGcagaggctgagtcgctgcat-3' (down) for m⁶A 2679, 5'-tagccagtaccgtagtgcgtgACTCCCTGTGGGCCAGTCCAGGA-3' (up) and 5'-5phos/CTGGGAGCCCTGGAGG CCCCTcagaggctgagtcgctgcat-3' (down) for A 2672. The sequences of the primers used for qPCR for SELECT were5'-ATGCAGCGACTCAGCCTCTG-3' (sense) and 5'-TAGCCAGTACCGTAGTGCGTG-3' (antisense).[45]

Construction and Transfection of Vectors and siRNAs

The cDNA encoding LEAWBIH was PCR-amplified using PrimeSTAR Max DNA Polymerase (cat. no. R045Q; Takara, Shiga, Japan) and primers 5'-TTGGTACCGAGCTCGGATCCTATATGTGAAGTGGGCGGTTG-3' (sense) and 5'-GGGTTTAAACGGGCCCTCTAGATTGTTTTGTTTGGTTGGTTTTATTT-3' (antisense). The PCR products were cloned into the *Bam*H I and *Xba* I sites of the pcDNA3.1(+) vector (Invitrogen) using the NovoRec Plus One-step PCR Cloning Kit (Novoprotein, Shanghai, China) to construct the LEAWBIH expression vector pcDNA3.1-LEAWBIH. The m⁶A-modified 2095 and 2679 site-mutated LEAWBIH expression vector pcDNA3.1-LEAWBIH-mut was constructed using the Fast Mutagenesis System (TransGen, Beijing, China) with the primers 5'-TGGAGAGATG ACAATGGTCTTGGACAAAG-3' (sense) and 5'-ACCATTGTCATCTCTCCAGCTAAGACAG-3' (antisense) for the mutation at the 2095 site, and 5'-GGCTCCCAGATCCTGGTCTGGCCCACAG-3' (sense) and 5'-ACCAGGATCT GGGAGCCCTGGAGGCCC-3' (antisense) for the mutation of 2679 site.

Two pairs of cDNA oligonucleotides targeting LEAWBIH were synthesized and cloned into the shRNA lentivirus expression vector (GenePharma, Shanghai, China), which was used to generate shRNA lentivirus targeting LEAWBIH. A scrambled non-targeting shRNA lentivirus was used as the negative control (NC). The shRNA oligonucleotide sequences were as follows:5'-GATCCGGGTTTCTCTGTGCCTGAAAGTTCAAGAGACTTTCAGGC ACAGAGAAACCCTTTTTTG-3' (sense) and 5'-AATTCAAAAAAGGGTTTCTCTGTGCCTGAAAGTCTCTTGA ACTTTCAGGCACAGAGAAACCCG-3' (antisense) for shRNA-LEAWBIH-1; 5-GATCCGGATGAAGAAACTTC TCATACTTCAAGAGAGTATGAGAAGTTTCTTCATCCTTTTTTG-3' (sense) and 5'-AATTCAAAAAAGGATGAAG AAACTTCTCATACTCTCTTGAAGTATGAGAAGTTTCTTCATCCG-3' (antisense) for shRNA-LEAWBIH-2; and 5-GATCCGTTCTCCGAACGTGTCACGTTTCAAGAGAACGTGACACGTTCGGAGAACTTTTTTG-3' (sense) and

5'-AATTCAAAAAAGTTCTCCGAACGTGTCACGTTCTCTTGAAACGTGACACGTTCGGAGAACG-3' (antisense) for shRNA-NC.

The METTL3 and FTO expression vectors were obtained from GenePharma (Shanghai, China). ON-TARGETplus Human YTHDC1 siRNA SMART Pool (Cat. no. L-015332-02-0010) and ON-TARGETplus Human KDM3B siRNA SMART Pool (cat. no. L-020378-01-0010) were purchased from Horizon Discovery (Cambridge, UK). Transfection of the vectors and siRNAs was performed using GP-transfect-Mate (GenePharma).

Construction of Stable Cell Lines

To construct HCC cells with stable overexpression of wild-type or m^{6}A-modified 2095 and 2679 sites mutated LEAWBIH, pcDNA3.1-LEAWBIH or pcDNA3.1-LEAWBIH-mut were transfected into HuH-7 and SK-HEP-1 cells. Forty-eight hours later, the cells were treated with 800 µg/ml G418 (InvivoGen, San Diego, CA, USA) for four weeks to select stably overexpressing cells. To construct HCC cells with stable knockdown of LEAWBIH, shRNA lentivirus targeting LEAWBIH was transfected into HuH-7 and Hep3B cells. Ninety-six hours later, the cells were treated with 2 µg/ml puromycin (InvivoGen) for four weeks to select for stably depleted cells.

Detection of Cell Proliferation, Migration, and Invasion

Glo cell viability and 5-ethynyl-2'-deoxyuridine (EdU) incorporation assays were performed to evaluate cell proliferation. Cell viability assays were performed using the CellTiter-Glo Luminescent Cell Viability Assay (Promega, Madison, WI, USA), as previously described.[46] EdU incorporation assay was carried out using the Cell-Light EdU Apollo567 In Vitro Kit (cat. no. C10310-1; RiboBio, Guangzhou, China) as previously described.[47–49] Transwell migration and invasion assays were conducted to evaluate cell migration and invasion as we previously described.[47–49]

Dual-Luciferase Reporter Assay

The β-catenin reporter TOPflash (Addgene, Watertown, MA, USA), which expresses firefly luciferase, and pRL-TK (Promega), which expresses Renilla luciferase, were cotransfected into the indicated cells. After transfection for 48h, firefly and Renilla luciferase activities were detected using the Dual-Luciferase Reporter Assay System (Promega).

Chromatin Isolation by RNA Purification (ChIRP) Assay

The ChIRP assay was conducted in HuH-7 cells using the EZ-Magna ChIRP RNA Interactome Kit (cat. no. 17–10495, Millipore). The sequences of the LEAWBIH antisense DNA probes were as follows:1, 5'-gtgagccagaggtcaatgaa-3'; 2, 5'-cccaccaagtcagaaagatg-3'; 3, 5'-aaattggggctcaagccaac-3'; 4, 5'-gaggggacccagcagaaaga-3'; 5, 5'-caagacagtcgcatgtatcc-3'; 6, 5'-tcatctttcaggcacagaga-3'; 7, 5'-gcctggaaggcaggaaaaag-3'; 8, 5'-aggaaatgtctgagctgtgg-3'; 9, 5'-ctcatgtggcagggaaaact-3'; 10, 5'-ctgcccagcattctaataaa-3'; 11, 5'-atttggaatctcttccacgg-3'; 12, 5'-taaaggccaaggtcagcata-3'; 13, 5'-ctaagacagcttacttggct-3'; 14, 5'-taggagaaggggcttcgaag-3'; 15, 5'-tggacctgcagaatgagctg-3'; 16, 5'-catgcatgtctccatattcc-3'; 17, 5'-tctcatgaatgacgcatgcg-3'; 18, 5'-ttatgggaagatccaggagg-3'; 19, 5'-ttcaacctggggagtgacag-3'; 20, 5'-atatgaggctgtgcagagag-3'. The enriched DNA was measured using qPCR with the following primers:5'-TGGGACAGGGGAGGATAC-3' (sense) and 5'-GGGCGG TGGAAAGTAGTC-3' (antisense) for *CTNNB1* promoter; 5'-GACGCTTTCTTTCCTTTCGC-3' (sense) and 5'-CTGCC CATTCATTTCCTTCC-3' (antisense) for *GAPDH* promoter.

Chromatin Immunoprecipitation (ChIP) Assay

The ChIP assay was conducted in indicated cells using the EZ-Magna ChIP A/G Chromatin Immunoprecipitation Kit (cat. no. 17–10086, Millipore) and H3K9me2 antibody (cat. no. ab1220, Abcam, Cambridge, MA, USA) or a KDM3B antibody (cat. no. 5377; Cell Signaling Technology, Danvers, MA). The enriched DNA was measured using qPCR with the primers5'-TGGGACAGGGGAGGATAC-3' (sense) and 5'-GGGCGGTGGAAAGTAGTC-3' (antisense) for *CTNNB1* promoter.

Statistical Analysis

Statistical analyses were performed using GraphPad Prism 6.0 Software. The Mann-Whitney test, Wilcoxon matched-pairs signed rank test, log-rank test, Student's t-test, one-way ANOVA followed by Dunnett's multiple comparisons test, Pearson's chi-square test, and Spearman's correlation analysis were conducted as indicated in the figure and table legends. Statistical significance was set at $P < 0.05$.

Results

High Expression of LEAWBIH in HCC and Its Correlation with Poor Survival of HCC Patients Were Identified

The correlation between LEAWBIH expression and prognosis was analyzed using the online tool GEPIA (Gene Expression Profiling Interactive Analysis, http://gepia.cancer-pku.cn/) based on TCGA-LIHC RNA-seq data. The results showed that high expression of LEAWBIH was correlated with short overall survival in patients with HCC (Figure 1A). LEAWBIH expression levels were analyzed using TCGA-LIHC RNA-seq data, and the results showed that high expression of LEAWBIH was found in HCC tissues compared to that in normal liver tissues (Figure 1B). TCGA-LIHC RNA-seq data also showed that stage III–IV have higher expression of LEAWBIH than stage I–II HCCs (Figure 1C). To further investigate the clinical relevance of LEAWBIH, we measured LEAWBIH expression in our HCC cohort, comprising 73 pairs of HCC tissues and matched adjacent noncancerous
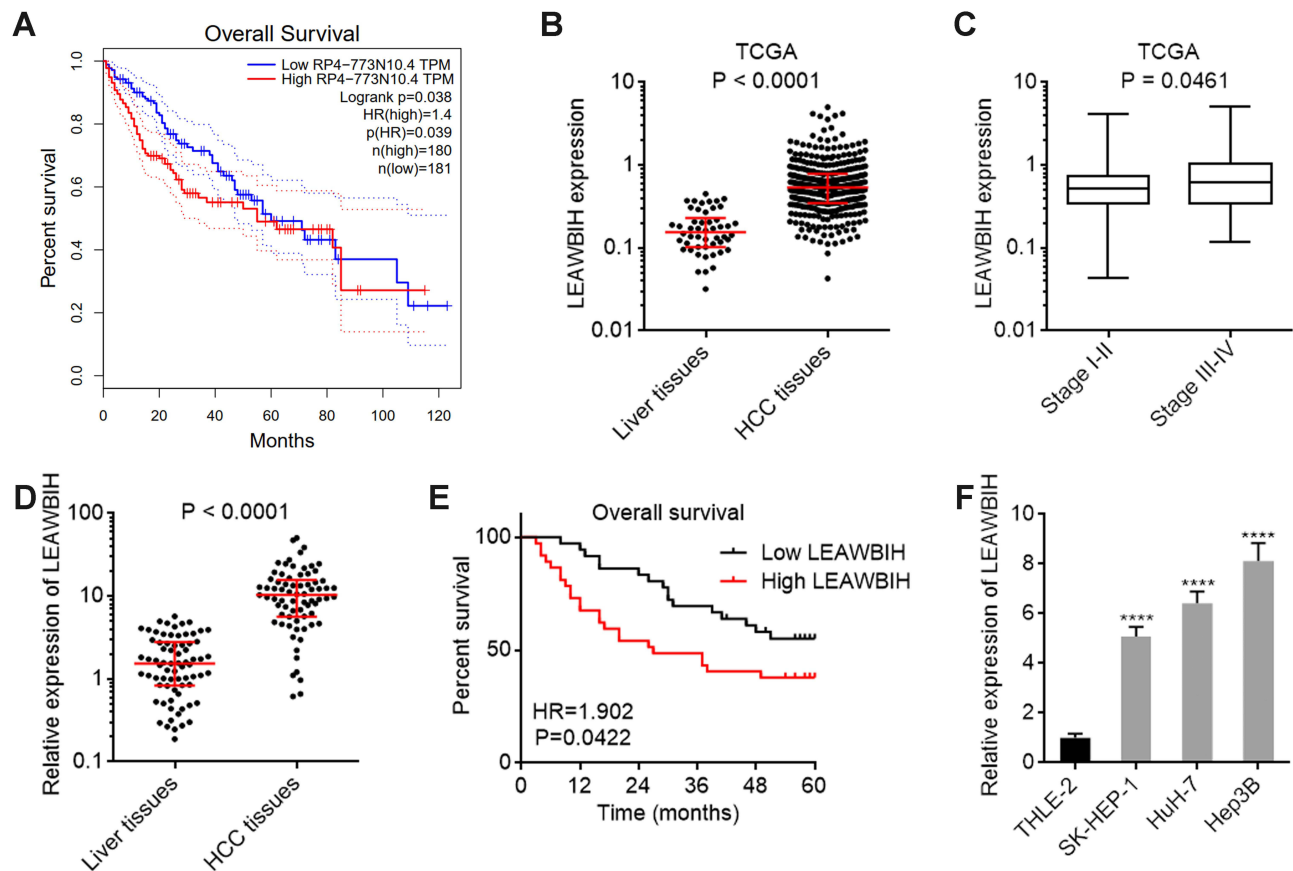

Figure 1 LEAWBIH was increased and correlated with poor overall survival in HCC. (**A**) The correlation between LEAWBIH (RP4-773N10.4) expression and overall survival based on the TCGA-LIHC RNA-seq data, analysed by the online tool GEPIA. (**B**) LEAWBIH expression in 371 HCC tissues and 50 normal liver tissues, based on the TCGA-LIHC RNA-seq data. Results are presented as median with interquartile range. P < 0.0001 by Mann-Whitney test. (**C**) LEAWBIH expression in 257 HCC tissues with stage I–II, and 90 HCC tissues with stage III–IV, based on the TCGA-LIHC RNA-seq data. Results are presented as median with interquartile range. P = 0.0461 by Mann-Whitney test. (**D**) LEAWBIH expression in 73 pairs of HCC tissues and matched adjacent liver tissues was measured by qPCR. Results are presented as median with interquartile range. P < 0.0001 by Wilcoxon matched-pairs signed rank test. (**E**) Kaplan-Meier survival analysis of the correlation between LEAWBIH expression and overall survival in our HCC cohort containing 73 cases. HR = 1.902, P = 0.0422 by log-rank test. (**F**) LEAWBIH expression in immortalized liver cell line THLE-2 and HCC cell lines SK-HEP-1, HuH-7, and Hep3B was measured by qPCR. Results are presented as mean ± standard deviation (SD) of 3 independent experiments. ****P < 0.0001 by one-way ANOVA followed by Dunnett's multiple comparisons test.

liver tissues. The results showed that LEAWBIH was more highly expressed in HCC tissues than in the liver tissues (Figure 1D). Kaplan-Meier survival analysis showed that high LEAWBIH expression was also correlated with short overall survival in our HCC cohort (Figure 1E). Furthermore, high expression of LEAWBIH was also found in the HCC cell lines SK-HEP-1, HuH-7, and Hep3B compared to that in the immortalized human liver cell line THLE-2 (Figure 1F).

m^{6}A Modification Upregulated LEAWBIH Expression via Increasing LEAWBIH Transcript Stability

LEAWBIH has been reported as an m^{6}A-related lncRNA in lower-grade glioma.[50] To investigate whether LEAWBIH was m^{6}A-modified in HCC, we performed a MeRIP assay in SK-HEP-1, HuH-7, and Hep3B cells. The results showed that m^{6}A-modified LEAWBIH was detected in all HCC cells (Figure 2A). The online tool SRAMP (http://www.cuilab.cn/
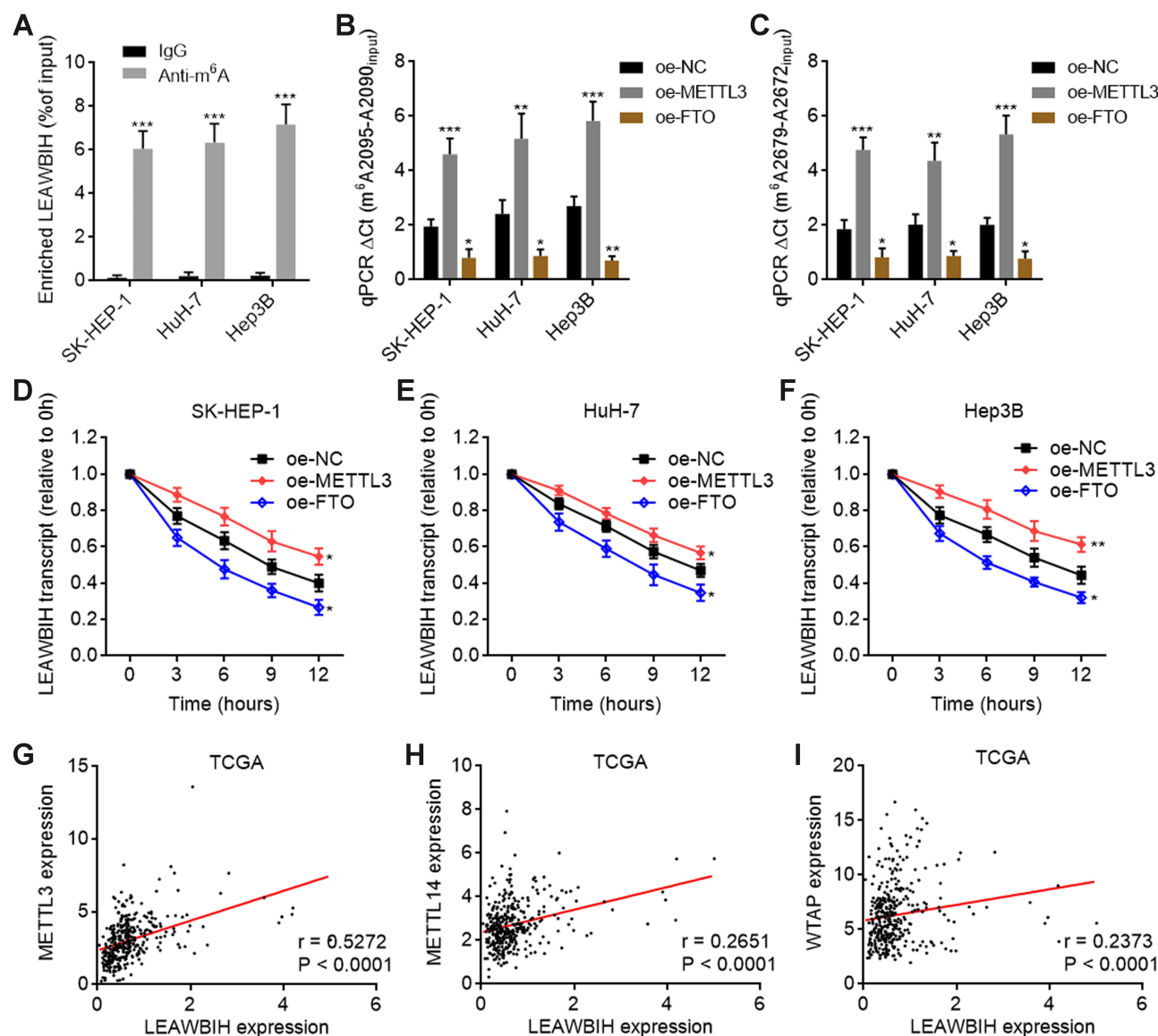

Figure 2 m^{6}A modification increased LEAWBIH transcript stability. (**A**) MeRIP assays followed by qPCR were performed in SK-HEP-1, HuH-7, and Hep3B cells to detect m^{6}A-modified LEAWBIH. (**B** and **C**) m^{6}A modification levels of 2095 (**B**) and 2679 (**C**) sites of LEAWBIH in SK-HEP-1, HuH-7, and Hep3B cells with METTL3 or FTO overexpression were measured by SELECT. (**D–F**) LEAWBIH transcript stability over time was measured after blocking new RNA synthesis with α-amanitin (50 μM) in SK-HEP-1 (**D**), HuH-7 (**E**) or Hep3B (**F**) cells with METTL3 or FTO overexpression. For (**A–F**), results are presented as mean ± SD of 3 independent experiments. *P < 0.05, **P < 0.01, ***P < 0.001 by Student's *t*-test (A) or one-way ANOVA followed by Dunnett's multiple comparisons test (B-F). (**G–I**) The correlation between LEAWBIH expression and METTL3 (**G**), METTL14 (**H**), or WTAP (**I**) expression in 371 HCC tissues, based on the TCGA-LIHC RNA-seq data. r and P values were calculated by Spearman correlation analysis.

sramp) predicted two m⁶A modification sites on LEAWBIH: 2095 and 2679 sites (Supplementary Figure 1A and B). To site-specifically detect m⁶A modification sites at 2095 and 2679 sites, we carried out a previously reported single-base elongation- and ligation-based qPCR amplification method (SELECT) (Supplementary Figure 1C).[45] The results presented that 2095 and 2679 sites were m⁶A-modified in SK-HEP-1, HuH-7, and Hep3B cells, and m⁶A modification levels of both 2095 and 2679 sites were increased after overexpression of m⁶A methylase METTL3 and decreased after overexpression of m⁶A demethylase FTO (Figure 2B and C). RNA stability assay showed that overexpression of METTL3 increased the stability of the LEAWBIH transcript, whereas overexpression of FTO decreased the stability of LEAWBIH transcripts in SK-HEP-1, HuH-7, and Hep3B cells (Figure 2D–F), suggesting that m⁶A modification may positively regulate LEAWBIH levels. Consistent with this, TCGA-LIHC RNA-seq data showed that the expression of LEAWBIH was positively correlated with the expression of m⁶A methylases METTL3, METTL14, and WTAP (Figure 2G–I). Similar with LEAWBIH, METTL3, METTL14, and WTAP were also highly expressed in HCC tissues compared to that in normal liver tissues, according to TCGA-LIHC RNA-seq data (Supplementary Figure 2A–C).

Increased m⁶A Modification Level of LEAWBIH and Its Positive Correlation with Poor Survival of HCC Patients Were Identified

Considering the positive effects of m⁶A modification on LEAWBIH, we investigated the potential clinical relevance of the level of m⁶A modification of LEAWBIH in HCC. SELECT assays revealed that m⁶A modification levels at 2095 and 2679 sites of LEAWBIH were increased in HCC tissues compared to those in paired adjacent liver tissues (Figure 3A and B). Kaplan-Meier survival analyses showed that high m⁶A modification levels at 2095 and 2679 sites were correlated with poor overall survival of patients with HCC (Figure 3C and D). Consistent with the positive regulation of LEAWBIH by m⁶A modification, m⁶A modification levels at sites 2095 and 2679 were positively correlated with LEAWBIH expression in HCC tissues (Figure 3E and F). Furthermore, m⁶A modification levels at 2095 and 2679 sites were increased in the HCC cell lines SK-HEP-1, HuH-7, and Hep3B compared with the immortalized human liver cell line THLE-2 (Figure 3G and H).

LEAWBIH Exerted Oncogenic Roles in HCC in an m⁶A Modification Dependent Manner

Because of the significant prognostic correlation between the expression and m⁶A modification of LEAWBIH in HCC, we investigated the potential functions of LEAWBIH in HCC. We generated HuH-7 and SK-HEP-1 cells with stable over-expression of wild-type or m⁶A-modified 2095 and 2679 sites mutated LEAWBIH (Figure 4A and B). Glo cell viability assays showed that HuH-7 and SK-HEP-1 cells overexpressing wild-type LEAWBIH had increased cell viability compared to control cells, which was abolished by mutation of the m⁶A-modified 2095 and 2679 sites of LEAWBIH (Figure 4C and D). EdU incorporation assays showed that HuH-7 and SK-HEP-1 cells with wild-type LEAWBIH overexpression had increased cell proliferation compared with control cells, which was also abolished by the mutation of the m⁶A-modified 2095 and 2679 sites of LEAWBIH (Figure 4E). Transwell migration and invasion assays showed that HuH-7 and SK-HEP-1 cells with wild-type LEAWBIH overexpression had increased cell migration and invasion compared with control cells, which were abolished by mutation of the m⁶A-modified 2095 and 2679 sites of LEAWBIH (Figure 4F and G). These data suggested that LEAWBIH exerts oncogenic effects in an m⁶A modification-dependent manner.

Knockdown of LEAWBIH Exerted Tumor Suppressive Roles in HCC

To further confirm the role of LEAWBIH in HCC, we generated HuH-7 and Hep3B cells with stable LEAWBIH knockdown (Figure 5A and B). Glo cell viability assays showed that HuH-7 and Hep3B cells with LEAWBIH knockdown had decreased cell viability compared to control cells (Figure 5C and D). EdU incorporation assays showed that HuH-7 and Hep3B cells with LEAWBIH knockdown had decreased proliferation compared with control cells (Figure 5E). Transwell migration and invasion assays showed that HuH-7 and Hep3B cells with LEAWBIH knockdown had decreased cell migration and invasion compared to the control cells (Figure 5F and G). These data suggest that knockdown of LEAWBIH exerts tumor-suppressive effects on HCC.

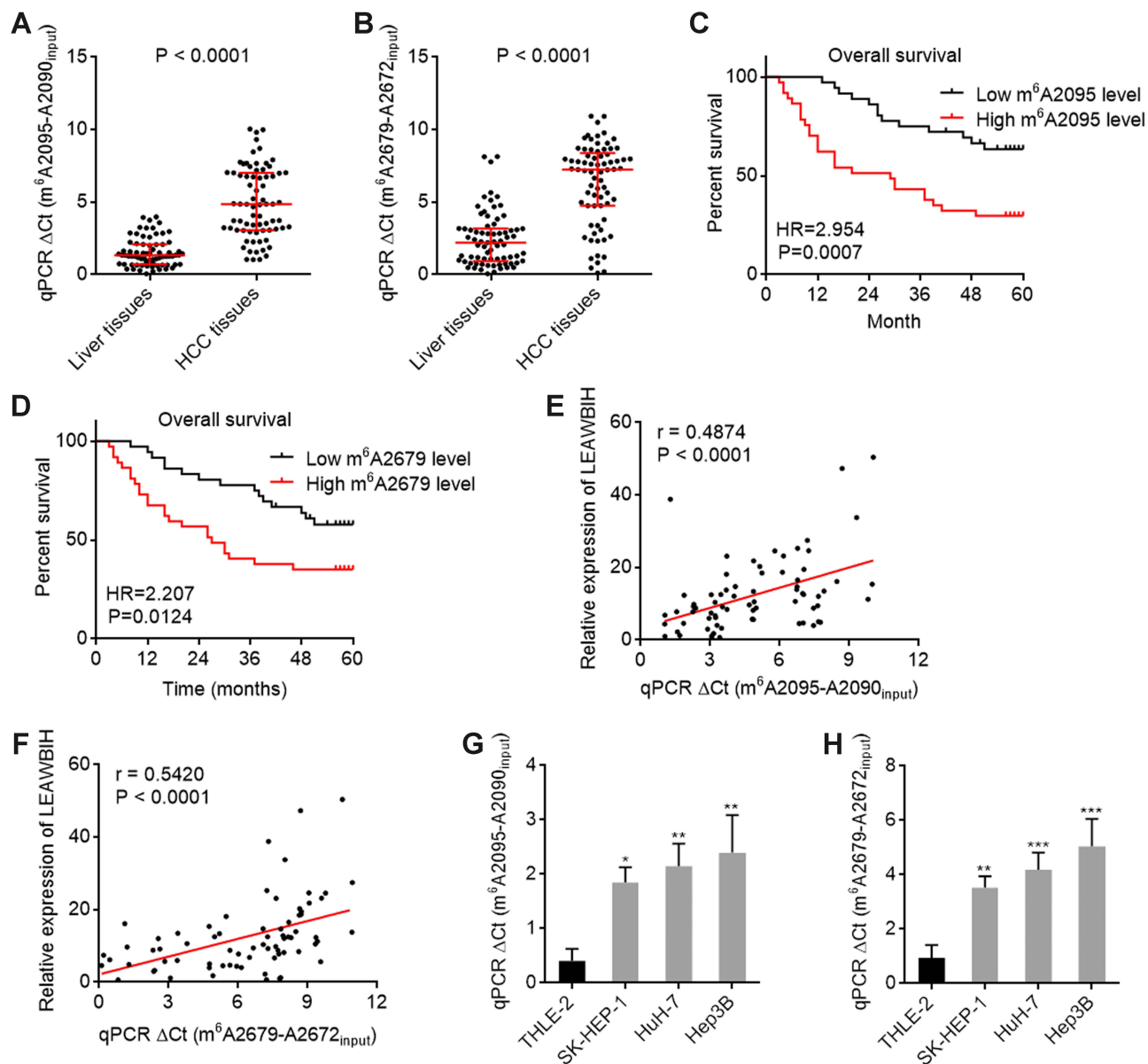**Figure 3** m[6]A modification level of LEAWBIH was increased and correlated with poor overall survival in HCC. (**A** and **B**) m[6]A modification levels of 2095 (**A**) and 2679 (**B**) sites of LEAWBIH in 73 pairs of HCC tissues and matched adjacent liver tissues was measured by SELECT. Results are presented as median with interquartile range. P < 0.0001 by Wilcoxon matched-pairs signed rank test. (**C** and **D**) Kaplan-Meier survival analysis of the correlation between m[6]A modification levels of 2095 (**C**) and 2679 (**D**) sites of LEAWBIH and overall survival in our HCC cohort containing 73 cases. HR and P values were calculated by log-rank test. (**E** and **F**) The correlation between LEAWBIH expression and m[6]A modification levels of 2095 (**E**) or 2679 (**F**) sites of LEAWBIH in HCC tissues. n = 73, r and P values were calculated by Spearman correlation analysis. (**G** and **H**) m[6]A modification levels of 2095 (**G**) and 2679 (**H**) sites of LEAWBIH in immortalized liver cell line THLE-2 and HCC cell lines SK-HEP-1, HuH-7, and Hep3B was measured by SELECT. Results are presented as mean ± SD of 3 independent experiments. *P < 0.05, **P < 0.01, ***P < 0.001 by one-way ANOVA followed by Dunnett's multiple comparisons test.

LEAWBIH Activated Wnt/β-Catenin Signaling in an m[6]A-Dependent Manner

To reveal the mechanisms responsible for the oncogenic roles of m[6]A-modified LEAWBIH in HCC, we performed Gene Set Enrichment Analysis (GSEA) of the TCGA-LIHC RNA-seq data. The TCGA-LIHC cohort was divided into a LEAWBIH high-expression group and LEAWBIH low-expression group based on the median LEAWBIH expression level. GSEA results presented that genes from "subtype S1" signature of HCC were significantly enriched in LEAWBIH high expression group (Figure 6A). Subclass S1 of HCC indicates aberrant activation of the Wnt/β-catenin signaling.[51] Thus, we further investigated the correlation between LEAWBIH and Wnt/β-catenin signaling using GSEA of TCGA-LIHC RNA-seq data. The results showed that several Wnt/β-catenin signaling gene signatures were significantly enriched
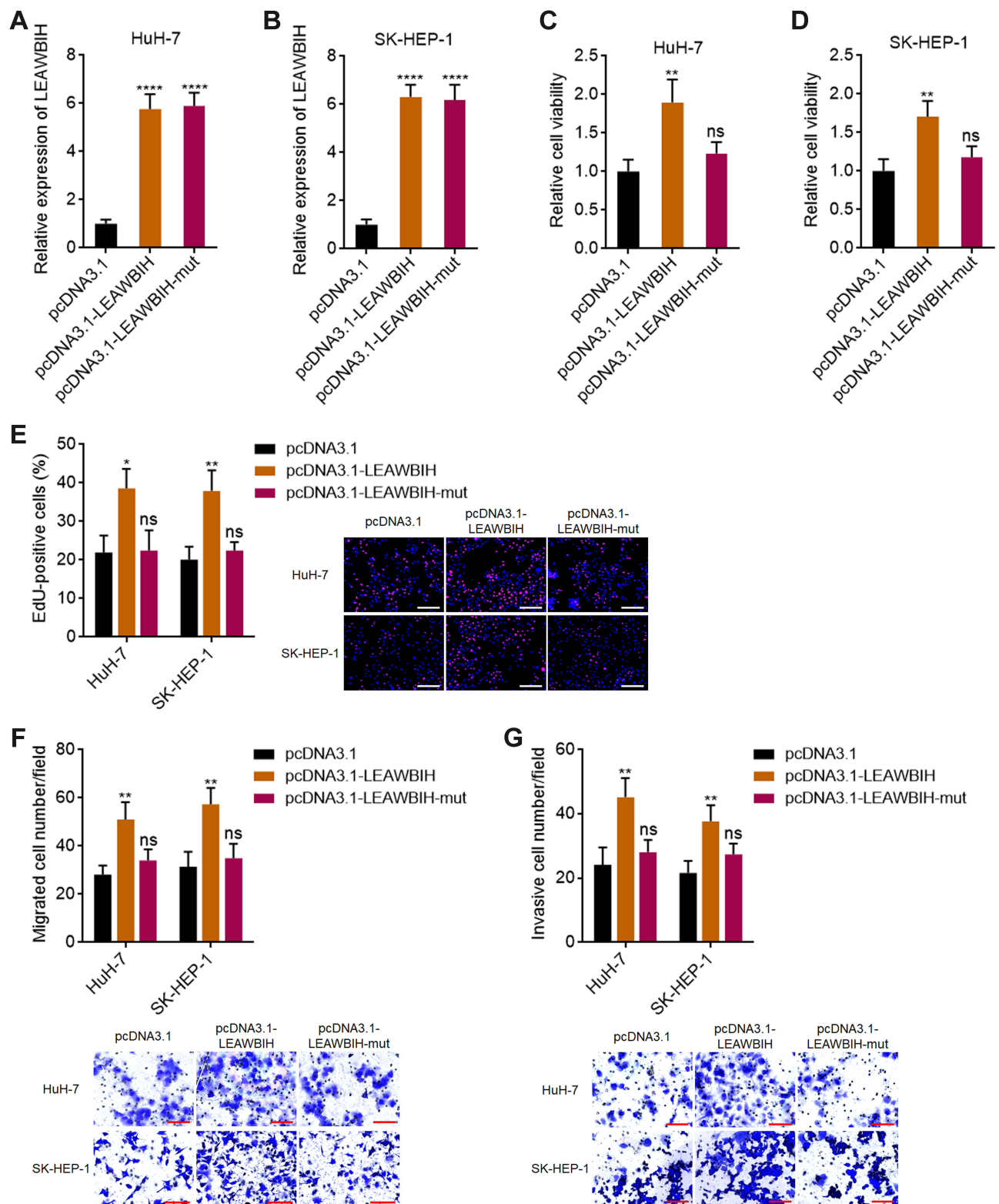
Figure 4 LEAWBIH promoted cell proliferation, migration, and invasion in an m⁶A dependent manner. (**A** and **B**) LEAWBIH expression in HuH-7 (**A**) and SK-HEP-1 (**B**) cells with stable overexpression of wild-type or m⁶A-modified 2095 and 2679 sites mutated LEAWBIH was detected by qPCR. (**C** and **D**) Cell viability of HuH-7 (**C**) and SK-HEP-1 (**D**) cells with overexpression of wild-type or mutated LEAWBIH was measured by Glo cell viability assay. (**E**) Cell proliferation of HuH-7 and SK-HEP-1 cells with overexpression of wild-type or mutated LEAWBIH was measured by EdU incorporation assay. Scale bars, 200 μm. (**F**) Cell migration of HuH-7 and SK-HEP-1 cells with overexpression of wild-type or mutated LEAWBIH was measured by transwell migration assay. Scale bars, 100 μm. (**G**) Cell invasion of HuH-7 and SK-HEP-1 cells with overexpression of wild-type or mutated LEAWBIH was measured by transwell invasion assay. Scale bars, 100 μm. Results are presented as mean ± SD of 3 independent experiments. *P < 0.05, **P < 0.01, ****P < 0.0001, ns, not significant, by one-way ANOVA followed by Dunnett's multiple comparisons test.
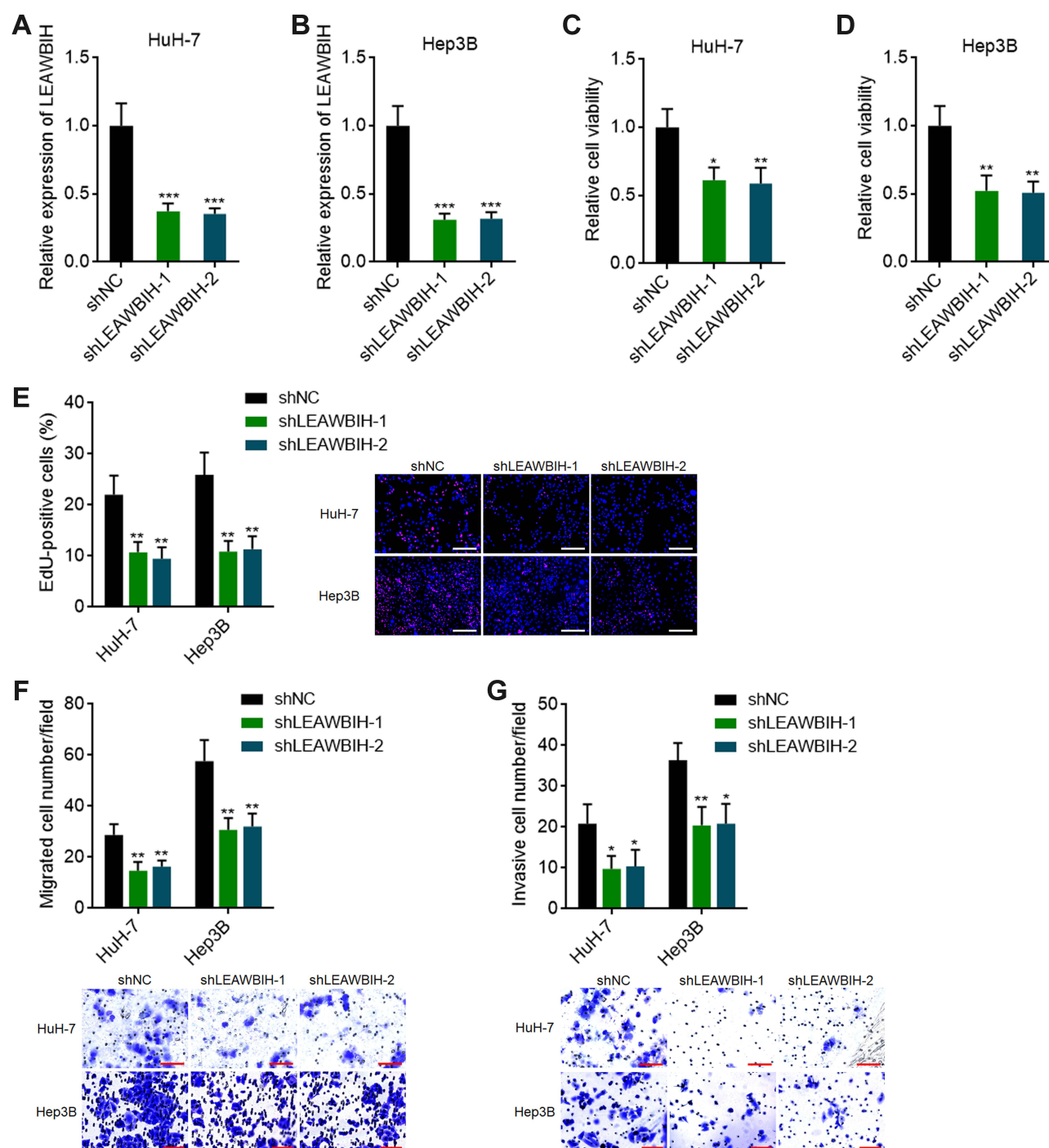
Figure 5 Knockdown of LEAWBIH repressed cell proliferation, migration, and invasion. (**A** and **B**) LEAWBIH expression in HuH-7 (**A**) and Hep3B (**B**) cells with stable knockdown of LEAWBIH was detected by qPCR. (**C** and **D**) Cell viability of HuH-7 (**C**) and Hep3B (**D**) cells with knockdown of LEAWBIH was measured by Glo cell viability assay. (**E**) Cell proliferation of HuH-7 and Hep3B cells with knockdown of LEAWBIH was measured by EdU incorporation assay. Scale bars, 200 μm. (**F**) Cell migration of HuH-7 and Hep3B cells with knockdown of LEAWBIH was measured by transwell migration assay. Scale bars, 100 μm. (**G**) Cell invasion of HuH-7 and Hep3B cells with knockdown of LEAWBIH was measured by transwell invasion assay. Scale bars, 100 μm. Results are presented as mean ± SD of 3 independent experiments. *$P < 0.05$, **$P < 0.01$, ***$P < 0.001$ by one-way ANOVA followed by Dunnett's multiple comparisons test.

in the LEAWBIH high expression group (Figure 6A). Therefore, we further investigated the potential effects of LEAWBIH on Wnt/β-catenin signaling. Dual-luciferase reporter assays showed that ectopic expression of LEAWBIH increased the luciferase activity of the β-catenin reporter TOPflash, which was abolished by mutation of the m6A-modified 2095 and 2679 sites of LEAWBIH (Figure 6B). Conversely, LEAWBIH knockdown decreased the
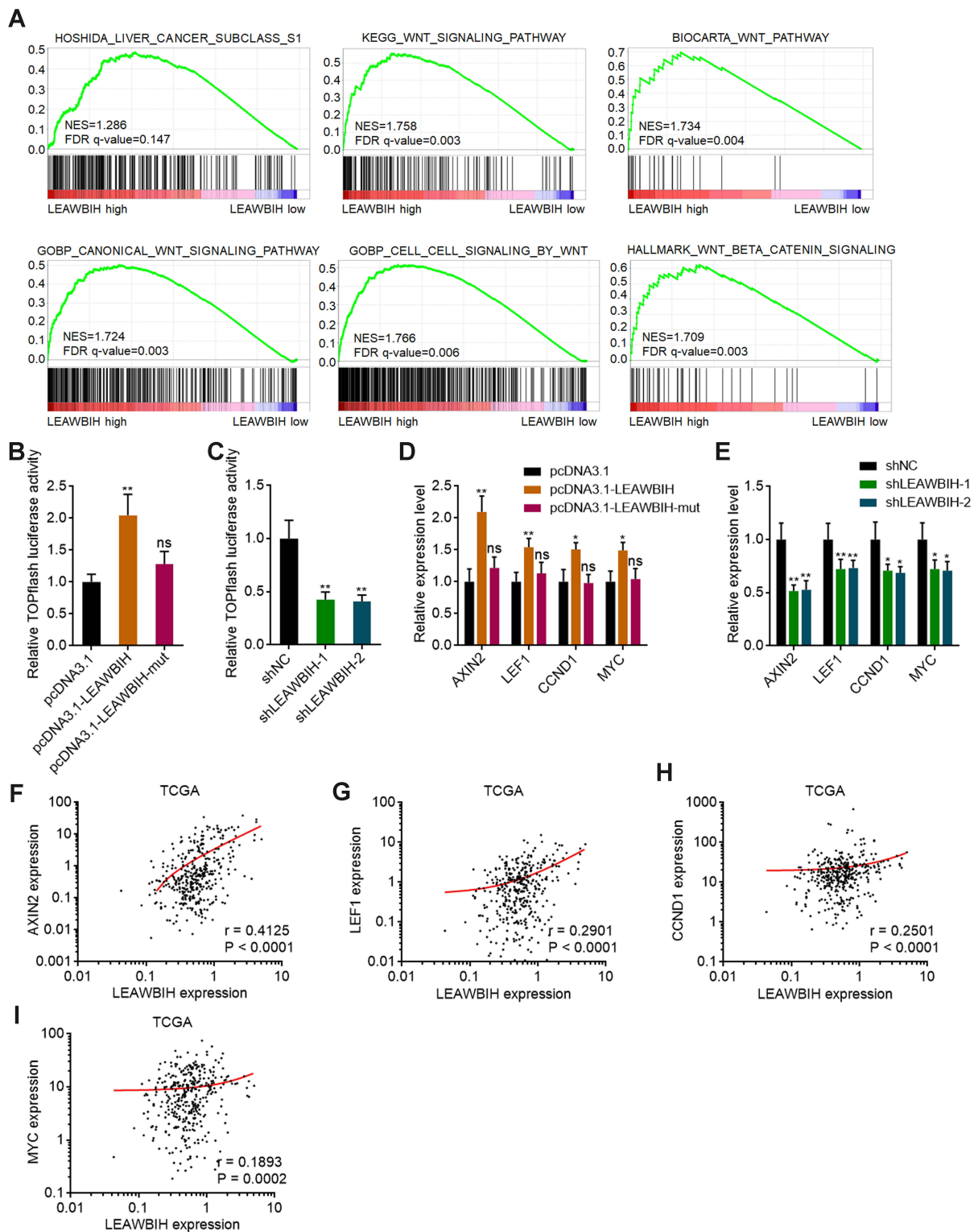
Figure 6 m[6]A-modified LEAWBIH activated Wnt/β-catenin signaling. (**A**) GSEA of HCC subclass S1 and Wnt/β-catenin signaling gene signatures in LEAWBIH high expression group versus LEAWBIH low expression group. NES, normalized enrichment score. (**B** and **C**) β-catenin reporter TOPFlash was co-transfected with pRL-TK into HuH-7 cells with overexpression of wild-type or mutated LEAWBIH (**B**) or HuH-7 cells with knockdown of LEAWBIH (**C**). Luciferase activities were measured 48 h after transfection. Results are presented as the relative ratio of firefly luciferase activity to Renilla luciferase activity. (**D**) The expression of Wnt/β-catenin targets in HuH-7 cells with overexpression of wild-type or mutated LEAWBIH was measured by qPCR. (**E**) The expression of Wnt/β-catenin signaling targets in HuH-7 cells with knockdown of LEAWBIH was measured by qPCR. For (**B–E**), results are presented as mean ± SD of 3 independent experiments. *P < 0.05, **P < 0.01, ns, not significant, by one-way ANOVA followed by Dunnett's multiple comparisons test. (**F–I**) The correlation between LEAWBIH expression and Wnt/β-catenin signaling targets AXIN2 (**F**), LEF1 (**G**), CCND1 (**H**), or MYC (**I**) expression in 371 HCC tissues, based on the TCGA-LIHC RNA-seq data. r and P values were calculated by Spearman correlation analysis.

luciferase activity of TOPflash (Figure 6C). Ectopic expression of LEAWBIH increased the expression of Wnt/β-catenin targets, including AXIN2, LEF1, CCND1, and MYC, which was also abolished by mutations in the m⁶A-modified 2095 and 2679 sites of LEAWBIH (Figure 6D). LEAWBIH knockdown decreased Wnt/β-catenin target expression (Figure 6E). TCGA-LIHC data revealed that LEAWBIH expression was positively correlated with the expression of Wnt/β-catenin targets (Figure 6F–I), further supporting the positive regulation of Wnt/β-catenin signaling by LEAWBIH. Similar with LEAWBIH, Wnt/β-catenin targets were also highly expressed in HCC tissues compared to that in normal liver tissues, according to TCGA-LIHC RNA-seq data (Supplementary Figure 2D and E).

m⁶A-Modified LEAWBIH Epigenetically Activated *CTNNB1* Expression Through Inducing Demethylation of H3K9me2 at *CTNNB1* Promoter Region

Analysis of TCGA-LIHC RNA-seq data also revealed a significant positive correlation between LEAWBIH and CTNNB1 (β-catenin encoding gene) expression (Figure 7A). Similar with LEAWBIH, CTNNB1 was also highly expressed in HCC tissues compared to that in normal liver tissues, according to TCGA-LIHC RNA-seq data (Supplementary Figure 2F). qPCR results showed that the expression of CTNNB1 was increased in HuH-7 cells overexpressing wild-type LEAWBIH, which was abolished by mutation of the m⁶A-modified 2095 and 2679 sites of LEAWBIH (Figure 7B). LEAWBIH decreased the expression of CTNNB1 (Figure 7C). These data suggest that LEAWBIH positively regulates CTNNB1 expression in an m⁶A dependent manner. Previous reports have shown that m⁶A-modified transcripts bind to the m⁶A reader YTHDC1, which further interacts with and recruits the H3K9me2 demethylase KDM3B, inducing H3K9me2 demethylation and gene activation.[52] To investigate whether m⁶A-modified LEAWBIH modulated *CTNNB1* transcription in such a manner, we first investigated whether LEAWBIH bound to *CTNNB1* promoter using the ChIRP assays. The results showed that LEAWBIH specifically bound to *CTNNB1* promoter (Figure 7D). ChIP assays showed that ectopic expression of LEAWBIH promoted the binding of KDM3B to *CTNNB1* promoter and decreased H3K9me2 levels at *CTNNB1* promoter, both of which were abolished by mutations in the m⁶A-modified 2095 and 2679 sites of LEAWBIH (Figure 7E). Knockdown of LEAWBIH reduced the binding of KDM3B to *CTNNB1* promoter and increased H3K9me2 levels at *CTNNB1* promoter (Figure 7F). The depletion of YTHDC1 abolished the effects of LEAWBIH on the binding of KDM3B to *CTNNB1* promoter and H3K9me2 levels at *CTNNB1* promoter (Figure 7G and Supplementary Figure 3A). Depletion of YTHDC1 also abolished the LEAWBIH-induced increase in *CTNNB1* expression (Figure 7H), suggesting that YTHDC1 is required for epigenetic roles of m⁶A-modified LEAWBIH in epigenetically activating *CTNNB1* expression. Similarly, KDM3B depletion abolished the LEAWBIH-induced increase in *CTNNB1* expression (Figure 7I and Supplementary Figure 3B). Collectively, these findings suggest that m⁶A-modified LEAWBIH epigenetically activates *CTNNB1* expression by inducing H3K9me2 demethylation at *CTNNB1* promoter region.

Blocking of Wnt/β-Catenin Signaling Reversed the Oncogenic Roles of LEAWBIH in HCC

To evaluate whether the oncogenic role of LEAWBIH in HCC is dependent on the activation of Wnt/β-catenin signaling, we treated LEAWBIH-overexpressing HuH-7 cells with the Wnt/β-catenin signaling inhibitor ICG-001 (Supplementary Figure 3C). Glo cell viability assays showed that ICG-001 treatment reversed the increase in cell viability caused by LEAWBIH overexpression (Figure 8A). EdU incorporation assays showed that treatment with ICG-001 reversed the increase in cell proliferation caused by LEAWBIH overexpression (Figure 8B). Transwell migration and invasion assays showed that treatment with ICG-001 reversed the increase in cell migration and invasion caused by LEAWBIH over-expression (Figure 8C and D). These data suggest that Wnt/β-catenin signalling activation is a critical mediator of the oncogenic role of LEAWBIH in HCC.

Discussion

As the most common RNA post-transcriptional modification, m⁶A plays an important role in determining RNA fate.[53] However, the clinical significance of m⁶A remains largely unclear. In this study, we found that the m⁶A modification
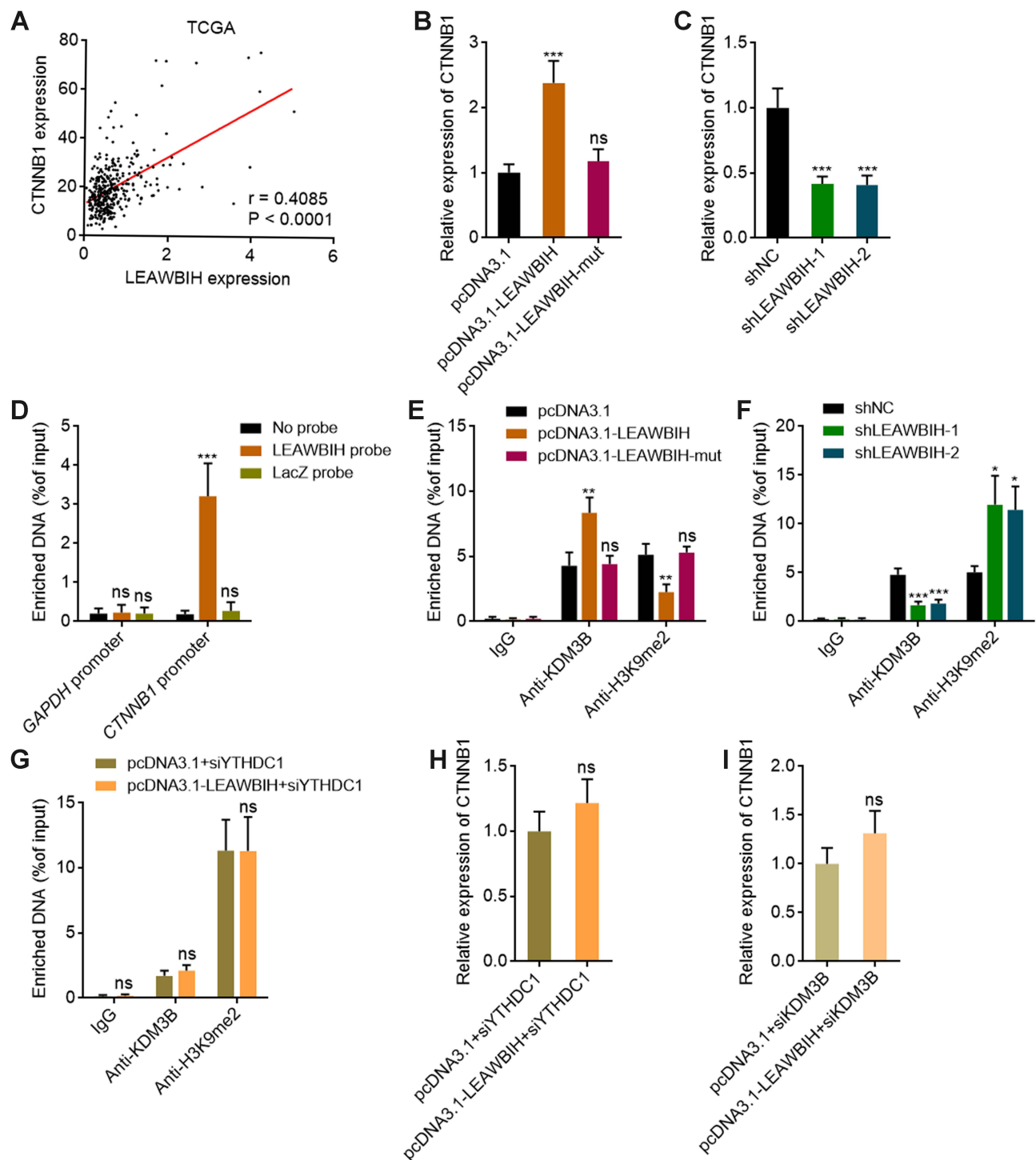
Figure 7 m[6]A-modified LEAWBIH epigenetically activated *CTNNB1* expression. (**A**) The correlation between LEAWBIH and CTNNB1 expression in 371 HCC tissues, based on the TCGA-LIHC RNA-seq data. r = 0.4085, P < 0.0001 by Spearman correlation analysis. (**B** and **C**) The expression of CTNNB1 in HuH-7 cells with overexpression of wild-type or mutated LEAWBIH (**B**) or HuH-7 cells with knockdown of LEAWBIH (**C**) was measured by qPCR. (**D**) ChIRP assays with LEAWBIH antisense probes or control probes were conducted in HuH-7 cells to measure the binding of LEAWBIH to *CTNNB1* promoter. *GAPDH* promoter was used as negative control. (**E**) ChIP assays with KDM3B or H3K9me2 specific antibodies were conducted in HuH-7 cells with overexpression of wild-type or mutated LEAWBIH to measure the binding of KDM3B to *CTNNB1* promoter and H3K9me2 level at *CTNNB1* promoter. (**F**) ChIP assays with KDM3B or H3K9me2 specific antibodies were conducted in HuH-7 cells with knockdown of LEAWBIH to measure the binding of KDM3B to *CTNNB1* promoter and H3K9me2 level at *CTNNB1* promoter. (**G**) ChIP assays with KDM3B or H3K9me2 specific antibodies were conducted in HuH-7 cells with overexpression of LEAWBIH and depletion of YTHDC1 to measure the binding of KDM3B to *CTNNB1* promoter and H3K9me2 level at *CTNNB1* promoter. (**H**) The expression of CTNNB1 in HuH-7 cells with overexpression of LEAWBIH and depletion of YTHDC1 was measured by qPCR. (**I**) The expression of CTNNB1 in HuH-7 cells with overexpression of LEAWBIH and depletion of KDM3B was measured by qPCR. Results are presented as mean ± SD of 3 independent experiments. *P < 0.05, **P < 0.01, ***P < 0.001, ns, not significant, by one-way ANOVA followed by Dunnett's multiple comparisons test (**B–F**) or Student's *t*-test (G-I).
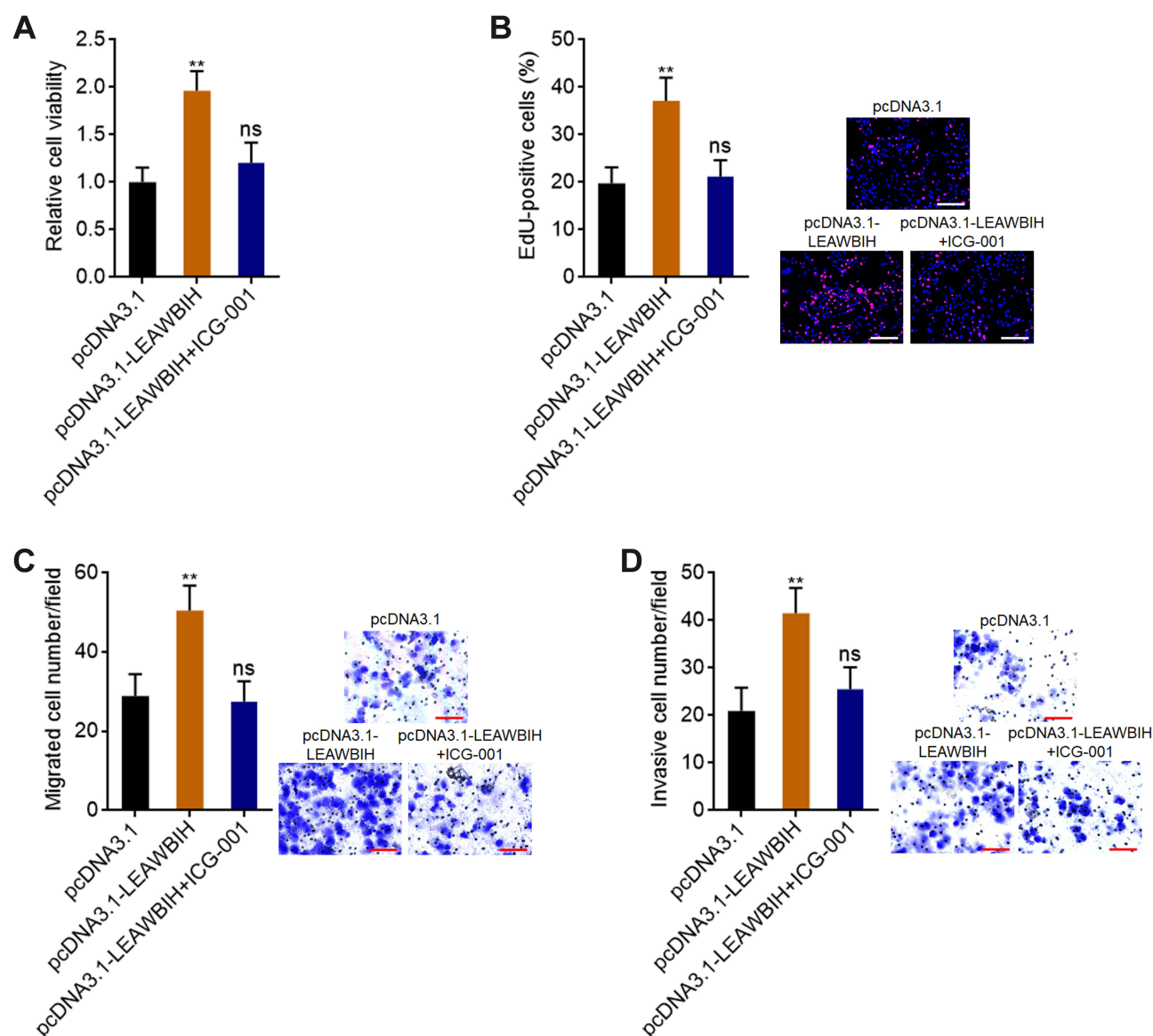
Figure 8 Blocking of Wnt/β-catenin signaling reversed the roles of LEAWBIH in promoting cell proliferation, migration, and invasion. (**A**) Cell viability of HuH-7 cells with overexpression of LEAWBIH treated with or without 5 μM ICG-001 was measured by Glo cell viability assay. (**B**) Cell proliferation of HuH-7 cells with overexpression of LEAWBIH treated with or without 5 μM ICG-001 was measured by EdU incorporation assay. Scale bars, 200 μm. (**C**) Cell migration of HuH-7 cells with overexpression of LEAWBIH treated with or without 5 μM ICG-001 was measured by transwell migration assay. Scale bars, 100 μm. (**D**) Cell invasion of HuH-7 cells with overexpression of LEAWBIH treated with or without 5 μM ICG-001 was measured by transwell invasion assay. Scale bars, 100 μm. Results are presented as mean ± SD of 3 independent experiments. **$P < 0.01$, ns, not significant, by one-way ANOVA followed by Dunnett's multiple comparisons test.

level of LEAWBIH is increased in HCC and increased m[6]A modification level of LEAWBIH predicts poor overall survival of patients with HCC. Furthermore, we found that the prognostic efficacy of m[6]A modification level in LEAWBIH was better than that in LEAWBIH. Thus, our findings suggest that m[6]A modification levels of specific transcripts may be prognostic biomarkers for specific diseases, such as the m[6]A modification level of LEAWBIH for HCCs' prognosis.

The m[6]A modification has been shown to have positive or negative roles in the stability of specific transcripts.[53] In this study, we found that m[6]A modification increases the stability of LEAWBIH. Thus, the m[6]A modification level of LEAWBIH positively correlated with its expression level. In addition to the effects of m[6]A modification on LEAWBIH stability, we found that the biological functions of LEAWBIH were influenced by m[6]A modification. LEAWBIH plays an oncogenic role in HCC by promoting cell proliferation, migration, and invasion. However, mutation of the m[6]A modification sites abolished the

oncogenic role of LEAWBIH. Our findings suggest that only m[6]A-modified LEAWBIH, but not unmodified LEAWBIH, plays oncogenic roles in HCC. These data revealed that m[6]A modification not only regulates RNA expression but also regulates RNA function.

Mechanistic investigations revealed that m[6]A-modified LEAWBIH binds to the m[6]A reader YTHDC1, which further interacts with and recruits the H3K9me2 demethylase KDM3B to *CTNNB1* promoter. H3K9me2 is a classical repressive histone mark.[54,55] By decreasing H3K9me2 levels in *CTNNB1* promoter region, m[6]A-modified LEAWBIH activates *CTNNB1* transcription. These findings provide novel evidence of the effects of m[6]A modifications on gene transcription. Previously, Li et al reported that m[6]A-modified transcripts interact with and recruit YTHDC1 and further KDM3B to the m[6]A-associated chromatin region, leading to the reduction of H3K9me2 and gene expression activation.[52] Deng et al reported that m[6]A-modified transcripts interact with another m[6]A reader FXR1, which further interacts with and recruits DNA 5-methylcytosine dioxygenase TET1 to genomic regions, leading to DNA demethylation and gene transcription.[56] All these findings revealed the interplays between RNA modification and epigenetic gene transcription.

CTNNB1 encodes β-catenin, which is a major component of the Wnt/β-catenin signaling pathway. Nuclear translocation of β-catenin activates the expression of Wnt/β-catenin downstream targets, which was routinely indicated as Wnt/β-catenin signaling activation.[57] Wnt/β-catenin signaling shows important roles in many pathophysiological processes.[58] In various cancers, Wnt/β-catenin signaling mainly shows tumor promotive roles.[59] In this study, we found that through epigenetic activation *CTNNB1* expression, m[6]A-modified LEAWBIH activated Wnt/β-catenin signaling, which is responsible for the oncogenic roles of m[6]A-modified LEAWBIH in HCC.

Conclusion

In conclusion, this study revealed that the m[6]A modification level of LEAWBIH was increased and correlated with a poor prognosis in HCC. m[6]A-modified LEAWBIH exerts oncogenic effects in HCC by epigenetically activating *CTNNB1* expression and Wnt/β-catenin signaling. These findings suggest that m[6]A-modified LEAWBIH is a potential therapeutic target for HCC.

Abbreviations

m[6]A, N[6]-methyladenosine; HCC, Hepatocellular carcinoma; lncRNA, long non-coding RNA; TCGA, The Cancer Genome Atlas; LIHC, Liver Hepatocellular Carcinoma; LEAWBIH, long non-coding RNA epigenetically activating Wnt/β-catenin signaling in HCC; FBS, fetal bovine serum; qPCR, quantitative polymerase chain reaction; cDNA, complementary DNA; MeRIP, methylated RNA immunoprecipitation; SELECT, single-base elongation- and ligation-based qPCR amplification method; NC, negative control; EdU,5-ethynyl-2'-deoxyuridine; ChIRP: Chromatin isolation by RNA purification; ChIP, Chromatin immunoprecipitation; GSEA, Gene Set Enrichment Analysis.

Ethics Approval and Consent to Participate

Human specimens were collected at the Affiliated Hospital of Youjiang Medical University for Nationalities. Written informed consent was obtained from all participants. This study was conducted in accordance with the Declaration of Helsinki and was reviewed and approved by the Affiliated Hospital of Youjiang Medical University for Nationalities Institutional Review Board.

Funding

Disclosure

The authors report no conflicts of interest in this work.

References

1. Sung H, Ferlay J, Siegel RL, et al. Global cancer statistics 2020: GLOBOCAN estimates of incidence and mortality worldwide for 36 cancers in 185 countries. *CA Cancer J Clin*. 2021;71:209–249. doi:10.3322/caac.21660

2. Llovet JM, Kelley RK, Villanueva A, et al. Hepatocellular carcinoma. *Nat Rev Dis Primers*. 2021;7:6. doi:10.1038/s41572-020-00240-3

3. Villanueva A. Hepatocellular Carcinoma. *N Engl J Med*. 2019;380:1450–1462. doi:10.1056/NEJMra1713263

4. Abou-Alfa GK, Meyer T, Cheng AL, et al. Cabozantinib in patients with advanced and progressing hepatocellular carcinoma. *N Engl J Med*. 2018;379:54–63. doi:10.1056/NEJMoa1717002

5. Ajoolabady A, Tang D, Kroemer G, Ren J. Ferroptosis in hepatocellular carcinoma: mechanisms and targeted therapy. *Br J Cancer*. 2023;128:190–205. doi:10.1038/s41416-022-01998-x

6. Baretti M, Kim AK, Anders RA. Expanding the immunotherapy roadmap for hepatocellular carcinoma. *Cancer Cell*. 2022;40:252–254. doi:10.1016/j.ccell.2022.02.017

7. Zheng X, Hou Z, Qian Y, et al. Tumors evade immune cytotoxicity by altering the surface topology of NK cells. *Nat Immunol*. 2023;24:802–813. doi:10.1038/s41590-023-01462-9

8. Liu T, Wang Z, Ye L, et al. Nucleus-exported CLOCK acetylates PRPS to promote de novo nucleotide synthesis and liver tumour growth. *Nat Cell Biol*. 2023;25:273–284. doi:10.1038/s41556-022-01061-0

9. Yuan JH, Liu XN, Wang TT, et al. The MBNL3 splicing factor promotes hepatocellular carcinoma by increasing PXN expression through the alternative splicing of lncRNA-PXN-AS1. *Nat Cell Biol*. 2017;19:820–832. doi:10.1038/ncb3538

10. Schulze K, Imbeaud S, Letouze E, et al. Exome sequencing of hepatocellular carcinomas identifies new mutational signatures and potential therapeutic targets. *Nat Genet*. 2015;47:505–511. doi:10.1038/ng.3252

11. Chen X, Cheung ST, So S, et al. Gene expression patterns in human liver cancers. *Mol Biol Cell*. 2002;13:1929–1939. doi:10.1091/mbc.02-02-0023

12. Andrisani O. Epigenetic mechanisms in hepatitis B virus-associated hepatocellular carcinoma. *Hepatoma Res*. 2021;7. doi:10.20517/2394-5079.2020.83

13. Sengupta I, Mondal P, Sengupta A, et al. Epigenetic regulation of Fructose-1,6-bisphosphatase 1 by host transcription factor Speckled 110 kDa during hepatitis B virus infection. *FEBS J*. 2022;289:6694–6713. doi:10.1111/febs.16544

14. Meunier L, Hirsch TZ, Caruso S, et al. DNA methylation signatures reveal the diversity of processes remodeling hepatocellular carcinoma methylomes. *Hepatology*. 2021;74:816–834. doi:10.1002/hep.31796

15. Zhu XT, Yuan JH, Zhu TT, Li YY, Cheng XY. Long noncoding RNA glypican 3 (GPC3) antisense transcript 1 promotes hepatocellular carcinoma progression via epigenetically activating GPC3. *FEBS J*. 2016;283:3739–3754. doi:10.1111/febs.13839

16. Zhao W, Mo H, Liu R, Chen T, Yang N, Liu Z. Matrix stiffness-induced upregulation of histone acetyltransferase KAT6A promotes hepatocellular carcinoma progression through regulating SOX2 expression. *Br J Cancer*. 2022;127:202–210. doi:10.1038/s41416-022-01784-9

17. Wang Y, Zeng J, Chen W, Fan J, Hylemon PB, Zhou H. Long Noncoding RNA H19: a novel oncogene in liver cancer. *Noncoding RNA*. 2023;9. doi:10.3390/ncrna9020019

18. Peng W, Bai S, Zheng M, et al. An exosome-related lncRNA signature correlates with prognosis, immune microenvironment, and therapeutic responses in hepatocellular carcinoma. *Transl Oncol*. 2023;31:101651. doi:10.1016/j.tranon.2023.101651

19. Zhang X, Jiang Q, Li J, et al. KCNQ1OT1 promotes genome-wide transposon repression by guiding RNA-DNA triplexes and HP1 binding. *Nat Cell Biol*. 2022;24:1617–1629. doi:10.1038/s41556-022-01008-5

20. Unfried JP, Ulitsky I. Substoichiometric action of long noncoding RNAs. *Nat Cell Biol*. 2022;24:608–615. doi:10.1038/s41556-022-00911-1

21. Beucher A, Miguel-Escalada I, Balboa D, et al. The HASTER lncRNA promoter is a cis-acting transcriptional stabilizer of HNF1A. *Nat Cell Biol*. 2022;24:1528–1540. doi:10.1038/s41556-022-00996-8

22. Li G, Kryczek I, Nam J, et al. LIMIT is an immunogenic lncRNA in cancer immunity and immunotherapy. *Nat Cell Biol*. 2021;23:526–537. doi:10.1038/s41556-021-00672-3

23. Li Y, Ding T, Hu H, et al. LncRNA-ATB participates in the regulation of calcium oxalate crystal-induced renal injury by sponging the miR-200 family. *Mol Med*. 2021;27:143. doi:10.1186/s10020-021-00403-2

24. Xia A, Yuan W, Wang Q, et al. The cancer-testis lncRNA lnc-CTHCC promotes hepatocellular carcinogenesis by binding hnRNP K and activating YAP1 transcription. *Nat Cancer*. 2022;3:203–218. doi:10.1038/s43018-021-00315-4

25. Yuan JH, Yang F, Wang F, et al. A long noncoding RNA activated by TGF-beta promotes the invasion-metastasis cascade in hepatocellular carcinoma. *Cancer Cell*. 2014;25:666–681. doi:10.1016/j.ccr.2014.03.010

26. Li S, Hu X, Yu S, et al. Hepatic stellate cell-released CXCL1 aggravates HCC malignant behaviors through the MIR4435-2HG/miR-506-3p/TGFB1 axis. *Cancer Sci*. 2023;114:504–520. doi:10.1111/cas.15605

27. Zhu N, Chen X, Zhao J, et al. Hypoxia-induced LINC00674 facilitates hepatocellular carcinoma progression by activating the NOX1/mTOR signaling pathway. *J Cancer*. 2022;13:3177–3188. doi:10.7150/jca.76458

28. Li JK, Chen C, Liu JY, et al. Long noncoding RNA MRCCAT1 promotes metastasis of clear cell renal cell carcinoma via inhibiting NPR3 and activating p38-MAPK signaling. *Mol Cancer*. 2017;16:111. doi:10.1186/s12943-017-0681-0

29. Ito-Kureha T, Leoni C, Borland K, et al. The function of Wtap in N(6)-adenosine methylation of mRNAs controls T cell receptor signaling and survival of T cells. *Nat Immunol*. 2022;23:1208–1221. doi:10.1038/s41590-022-01268-1

30. Wu Y, Xu X, Qi M, et al. N(6)-methyladenosine regulates maternal RNA maintenance in oocytes and timely RNA decay during mouse maternal-to-zygotic transition. *Nat Cell Biol*. 2022;24:917–927. doi:10.1038/s41556-022-00915-x

31. Xu Y, Lv D, Yan C, et al. METTL3 promotes lung adenocarcinoma tumor growth and inhibits ferroptosis by stabilizing SLC7A11 m(6)A modification. *Cancer Cell Int*. 2022;22:11. doi:10.1186/s12935-021-02433-6

32. Dong L, Chen C, Zhang Y, et al. The loss of RNA N(6)-adenosine methyltransferase Mettl14 in tumor-associated macrophages promotes CD8(+) T cell dysfunction and tumor growth. *Cancer Cell*. 2021;39:945–957 e10. doi:10.1016/j.ccell.2021.04.016

33. Weng H, Huang F, Yu Z, et al. The m(6)A reader IGF2BP2 regulates glutamine metabolism and represents a therapeutic target in acute myeloid leukemia. *Cancer Cell*. 2022;40:1566–1582. doi:10.1016/j.ccell.2022.10.004

34. Cheng Y, Xie W, Pickering BF, et al. N(6)-Methyladenosine on mRNA facilitates a phase-separated nuclear body that suppresses myeloid leukemic differentiation. *Cancer Cell*. 2021;39:958–972 e8. doi:10.1016/j.ccell.2021.04.017

35. Cai Z, Zhang Y, Yang L, et al. ALKBH5 in mouse testicular Sertoli cells regulates Cdh2 mRNA translation to maintain blood-testis barrier integrity. *Cell Mol Biol Lett*. 2022;27:101. doi:10.1186/s11658-022-00404-x

36. Zhang R, Qu Y, Ji Z, et al. METTL3 mediates Ang-II-induced cardiac hypertrophy through accelerating pri-miR-221/222 maturation in an m6A-dependent manner. *Cell Mol Biol Lett*. 2022;27:55. doi:10.1186/s11658-022-00349-1

37. Zhang X, Lu N, Wang L, et al. Recent advances of m(6)A methylation modification in esophageal squamous cell carcinoma. *Cancer Cell Int*. 2021;21:421. doi:10.1186/s12935-021-02132-2

38. Sun W, Li Y, Ma D, et al. ALKBH5 promotes lung fibroblast activation and silica-induced pulmonary fibrosis through miR-320a-3p and FOXM1. *Cell Mol Biol Lett*. 2022;27:26. doi:10.1186/s11658-022-00329-5

39. Du H, Zou NY, Zuo HL, Zhang XY, Zhu SC. YTHDF3 mediates HNF1alpha regulation of cervical cancer radio-resistance by promoting RAD51D translation in an m6A-dependent manner. *FEBS J*. 2022;290:1920–1935. doi:10.1111/febs.16681

40. Shimura T, Kandimalla R, Okugawa Y, et al. Novel evidence for m(6)A methylation regulators as prognostic biomarkers and FTO as a potential therapeutic target in gastric cancer. *Br J Cancer*. 2022;126:228–237. doi:10.1038/s41416-021-01581-w

41. Dai YZ, Liu YD, Li J, et al. METTL16 promotes hepatocellular carcinoma progression through downregulating RAB11B-AS1 in an m(6) A-dependent manner. *Cell Mol Biol Lett*. 2022;27:41. doi:10.1186/s11658-022-00342-8

42. Lan J, Xu B, Shi X, Pan Q, Tao Q. WTAP-mediated N(6)-methyladenosine modification of NLRP3 mRNA in kidney injury of diabetic nephropathy. *Cell Mol Biol Lett*. 2022;27:51. doi:10.1186/s11658-022-00350-8

43. Zhang M, Wang J, Jin Y, et al. YTHDF2-mediated FGF14-AS2 decay promotes osteolytic metastasis of breast cancer by enhancing RUNX2 mRNA translation. *Br J Cancer*. 2022;127:2141–2153. doi:10.1038/s41416-022-02006-y

44. Tang Z, Li C, Kang B, Gao G, Li C, Zhang Z. GEPIA: a web server for cancer and normal gene expression profiling and interactive analyses. *Nucleic Acids Res*. 2017;45:W98–W102. doi:10.1093/nar/gkx247

45. Xiao Y, Wang Y, Tang Q, Wei L, Zhang X, Jia G. An elongation- and ligation-based qPCR amplification method for the radiolabeling-free detection of locus-specific N(6) -methyladenosine modification. *Angew Chem Int Ed Engl*. 2018;57:15995–16000. doi:10.1002/anie.201807942

46. Liu XN, Yuan JH, Wang TT, Pan W, Sun SH. An alternative POLDIP3 transcript promotes hepatocellular carcinoma progression. *Bio Pharmacother*. 2017;89:276–283. doi:10.1016/j.biopha.2017.01.139

47. Wei H, Xu Z, Chen L, et al. Long non-coding RNA PAARH promotes hepatocellular carcinoma progression and angiogenesis via upregulating HOTTIP and activating HIF-1alpha/VEGF signaling. *Cell Death Dis*. 2022;13:102. doi:10.1038/s41419-022-04505-5

48. Pu J, Li W, Wang A, et al. Long non-coding RNA HOMER3-AS1 drives hepatocellular carcinoma progression via modulating the behaviors of both tumor cells and macrophages. *Cell Death Dis*. 2021;12:1103. doi:10.1038/s41419-021-04309-z

49. Pu J, Zhang Y, Wang A, et al. ADORA2A-AS1 restricts hepatocellular carcinoma progression via binding hur and repressing FSCN1/AKT axis. *Front Oncol*. 2021;11:754835. doi:10.3389/fonc.2021.754835

50. Tu Z, Wu L, Wang P, et al. N6-methylandenosine-related lncRNAs are potential biomarkers for predicting the overall survival of lower-grade glioma patients. *Front Cell Dev Biol*. 2020;8:642. doi:10.3389/fcell.2020.00642

51. Hoshida Y, Nijman SM, Kobayashi M, et al. Integrative transcriptome analysis reveals common molecular subclasses of human hepatocellular carcinoma. *Cancer Res*. 2009;69:7385–7392. doi:10.1158/0008-5472.CAN-09-1089

52. Li Y, Xia L, Tan K, et al. N(6)-Methyladenosine co-transcriptionally directs the demethylation of histone H3K9me2. *Nat Genet*. 2020;52:870–877. doi:10.1038/s41588-020-0677-3

53. Boulias K, Greer EL. Biological roles of adenine methylation in RNA. *Nat Rev Genet*. 2023;24:143–160. doi:10.1038/s41576-022-00534-0

54. Nachiyappan A, Gupta N, Taneja R. EHMT1/EHMT2 in EMT, cancer stemness and drug resistance: emerging evidence and mechanisms. *FEBS J*. 2022;289:1329–1351. doi:10.1111/febs.16334

55. Padeken J, Methot SP, Gasser SM. Establishment of H3K9-methylated heterochromatin and its functions in tissue differentiation and maintenance. *Nat Rev Mol Cell Biol*. 2022;23:623–640. doi:10.1038/s41580-022-00483-w

56. Deng S, Zhang J, Su J, et al. RNA m(6)A regulates transcription via DNA demethylation and chromatin accessibility. *Nat Genet*. 2022;54:1427–1437. doi:10.1038/s41588-022-01173-1

57. You H, Li Q, Kong D, et al. The interaction of canonical Wnt/beta-catenin signaling with protein lysine acetylation. *Cell Mol Biol Lett*. 2022;27:7. doi:10.1186/s11658-021-00305-5

58. Quandt J, Arnovitz S, Haghi L, et al. Wnt-beta-catenin activation epigenetically reprograms T(reg) cells in inflammatory bowel disease and dysplastic progression. *Nat Immunol*. 2021;22:471–484. doi:10.1038/s41590-021-00889-2

59. Li J, Li MH, Wang TT, et al. SLC38A4 functions as a tumour suppressor in hepatocellular carcinoma through modulating Wnt/beta-catenin/MYC/ HMGCS2 axis. *Br J Cancer*. 2021;125:865–876. doi:10.1038/s41416-021-01490-y